Available online at www.sciencedirect.com
SCIENCE DIRECT®
Journal of Organometallic Chemistry 690 (2005) 3044–3053
Journal of Organometallic Chemistry
www.elsevier.com/locate/jorganchem

Reactions of the unsaturated triosmium cluster $[(\mu\text{-H})Os_3(CO)_8(Ph_2PCH_2P(Ph)C_6H_4)]$ with HX (X = Cl, Br, F, CF_3CO_2,CH_3CO_2): X-ray structures of $[(\mu\text{-H})Os_3(CO)_7(\eta^1\text{-Cl})(\mu\text{-Cl})_2(\mu\text{-dppm})]$, $[(\mu\text{-H})_2Os_3(CO)_8(Ph_2PCH_2P(Ph)C_6H_4)]^+[CF_3O]^-$ and the two isomers of $[(\mu\text{-H})Os_3(CO)_8(\mu\text{-Cl})(\mu\text{-dppm})]$

Shariff E. Kabir [a,*], Md. Arzu Miah [a], Nitai C. Sarker [a], G.M. Golzar Hossain [b], Kenneth I. Hardcastle [c], Dalia Rokhsana [d], Edward Rosenberg [d,*]

[a] Department of Chemistry, Jahangirnagar University, Savar, Dhaka 1342, Bangladesh
[b] Department of Chemistry, Cardiff University, P.O. Box 912, Park Place, Cardiff CF10 3TB, UK
[c] Department of Chemistry, Emory University, Atlanta, GA 30322, USA
[d] Department of Chemistry, The University of Montana, 32 Campus Drive, Missoula, MT 59812, USA

Received 10 March 2005; revised 22 March 2005; accepted 22 March 2005
Available online 11 May 2005

Abstract

Treatment of the electronically unsaturated cluster $[(\mu\text{-H})Os_3(CO)_8(Ph_2PCH_2P(Ph)C_6H_4)]$ (**1**) with HCl gas at ambient temperature in dichloromethane afforded $(\mu\text{-H})Os_3(CO)_8(\mu\text{-Cl})(\mu\text{-dppm})$ (**2**) and $[(\mu\text{-H})Os_3(CO)_7(\eta^1\text{-Cl})(\mu\text{-Cl})_2(\mu\text{-dppm})]$ (**3**). Thermolysis of **2** at 110 °C led to an isomer of **2**, **4**. A similar reaction of **1** with HBr gas gave $[(\mu\text{-H})Os_3(CO)_8(\mu\text{-Br})(\mu\text{-dppm})]$ (**5**) as the only product which does not isomerize at 110 °C. In sharp contrast, treatment of **1** with HF gas gave the protonated species $[(\mu\text{-H})_2Os_3(CO)_8(Ph_2PCH_2P(Ph)C_6H_4)]^+$ (**6**). Treatment of **1** with CF_3CO_2H also gave cation **6** whereas CH_3CO_2H yielded $[(\mu\text{-H})Os_3(CO)_8(\mu\text{-}\eta^2\text{-}CH_3CO_2)(\mu\text{-dppm})]$ (**7**). Structures of **2**, **3**, **4** and **6** were established crystallographically. In **2**, both the chloride and the hydride ligands simultaneously bridge the same Os–Os edge and the dppm spans another Os–Os bond whereas in **4**, all the three ligands bridge the same Os–Os edge. Compound **3** is comprised of an open Os_3 arrangement in which one chloride bridges the open Os···Os edge, another chloride and a hydride mutually bridge an Os–Os bond and the third chloride is terminally coordinated to one of the Os atoms of the dppm bridged edge. The cation **6** consists of a triangle of osmium atoms in which the shortest Os–Os edge is bridged by a hydride and the metallated phenyl ring and the longest edge is bridged by another hydride and the diphosphine ligand.

Keywords: Triosmium clusters; Electronically unsaturated; Protic acid; Thermolysis; X-ray structures

1. Introduction

The reactions of triosmium carbonyl clusters with protic acids have been thoroughly investigated and found to exhibit a range of reactivity patterns [1–8].

* Corresponding authors. Tel.: +1 406 243 2592; fax: +1 406 243 4227.
E-mail addresses: skabir_ju@yahoo.com (S.E. Kabir), edward.rosenberg@mso.umt.edu (E. Rosenberg).

0022-328X/$ - see front matter © 2005 Elsevier B.V. All rights reserved.
doi:10.1016/j.jorganchem.2005.03.041

Most common is simple protonation to give cationic hydrido species in which the hydride adopts a bridging coordination site [1–5] although cleavage of a metal–carbon [6] or a metal–metal bond [7] are known to occur as well. For example, the parent compound $[Os_3(CO)_{12}]$ reacts with concentrated H_2SO_4 to give the cationic species $[(\mu\text{-}H)Os_3(CO)_{12}]^+$ [1]. The protonation of electron rich mono- and diphosphine derivatives occur more readily on treatment with weaker acids such as CF_3CO_2H. The unsaturated cluster $[(\mu\text{-}H)_2Os_3(CO)_{10}]$ and its tertiary phosphine substituted derivatives $[(\mu\text{-}H)_2Os_3(CO)_9(L)]$ (L = PEt_3, or PPh_3) react with CF_3CO_2H to give the cationic clusters $[(\mu\text{-}H)_3Os_3(CO)_{10}]^+$ and $[(\mu\text{-}H)_3Os_3(CO)_9L]^+$, respectively [8]. The cyclometallated compound $[(\mu\text{-}H)_2Os_3(CO)_9(\mu_3\text{-}P(C_6H_4)Ph)]$ reacts with Brønsted acids HX via a protonation followed by anion coordination to give the addition products $[(\mu\text{-}H)_2Os_3(X)(CO)_9(\mu\text{-}PPh_2)]$ (X = F, Cl, Br or CF_3CO_2) but with HBF_4 only the protonated complex $[(\mu\text{-}H)_3Os_3(CO)_9(\mu_3\text{-}P(C_6H_4)Ph)]^+$ is obtained [9]. In some cases, stable ploynuclear species where the acid's conjugate base has coordinated to the cluster in place of an organic ligand or a metal–metal bond can be isolated. For example, Shapley and co-workers [6] reported that the triflate compound $[(\mu\text{-}H)_2Os_3(CO)_9(O_3SCF_3)_2]$ reacts with CF_3CO_2H and CH_3CO_2H to afford the mixed oxyanion ligand clusters $[(\mu\text{-}H)_2Os_3(CO)_9(\mu,\eta^2\text{-}O_2CCF_3)_2(\eta^1\text{-}O_3SCF_3)]$ and $[(\mu\text{-}H)_2Os_3(CO)_9(\mu,\eta^2\text{-}O_2CCH)_2(\eta^1\text{-}O_3SCF_3)]$. We also reported that protonation of μ-vinyloxy ligand in $[(\mu\text{-}H)Os_3(CO)_{10}(\mu\text{-}OCH{=}CH_2)]$ with HX leads to the compounds $[(\mu\text{-}H)Os_3(CO)_{10}(\mu\text{-}X)]$ (X = Cl, CF_3CO_2) with liberation of aldehyde via the intermediate addition species $[(\mu\text{-}H)Os_3(CO)_{10}(\mu\text{-}OCHXCH_3)]$ [10]. Such acid adducts of the general formula $[(\mu\text{-}H)Os_3(CO)_{10}(\mu\text{-}X)]$ (X = RCO_2, halogen, MeO) are also available from the lightly stabilized cluster $[Os_3(CO)_{10}(MeCN)_2]$ [11,12]. A few years ago we reported the first example of direct adduct formation not accompanied by ligand displacement or metal–metal bond cleavage from the reactions of the μ_3-imidoyl cluster $[(\mu\text{-}H)Os_3(CO)_9(\mu_3\text{-}\eta^2\text{-}C{=}NCH_2CH_2CH_2\text{–})]$ with HX to afford $[(\mu\text{-}H)_2Os_3(CO)_9(\mu_3\text{-}\eta^2\text{-}C{=}NCH_2CH_2CH_2\text{–})]X$ (X = Cl, Br, CF_3CO_2, CF_3SO_3) [13]. We have recently reported [14] that the electron-deficient quinoline triosmium clusters $[(\mu\text{-}H)Os_3(CO)_9(\mu_3\text{-}\eta^2\text{-}XC_9H_6N)]$ (X = H, 5-NH_2, 6-NH_2, 3-NH_2, 5-Br, 5-CH_3) all undergo simple protonation with both coordinating (CF_3CO_2H) and non-coordinating acids (HBF_4).

The reactions of the coordinatively unsaturated triosmium cluster $[(\mu\text{-}H)Os_3(CO)_8(\mu_3\text{-}\eta^3\text{-}Ph_2PCH_2P(Ph)C_6H_4)]$ (**1**) with a wide variety of small inorganic and organic ligands such as CO [15], H_2[16], PR_3 [17], $P(OR)_3$ (R = Me, Et, Pr^i, Bu or Ph) [17], PPh_2H [18], RC≡CR (R = Ph, C_6H_4Me, Me or CF_3) [19], $[Au(PPh_3)]PF_6$ [20], EtSH [21], $CH_3CH(CH_3)SH$ [21], PhSH [21], pySH [22], $HSCH_2CH_2SH$ [23], $HSCH_2CH_2CH_2SH$ [23], and Se [24] that afford many interesting and potentially useful compounds have been investigated. Our recent studies of the reactivity of **1** toward CH_2CN_2 [25] and silanes [26] have uncovered some examples of its distinctly different reactivity patterns compared with unsaturated benzoheterocyclic triosmium clusters [27]. Herein, we report our results on the investigations of the reactions of **1** with a series of Brønsted acids. It was of interest to examine whether structurally diverse products would also be accessible in these systems.

2. Results and discussion

When HCl gas was bubbled through a dichloromethane solution of the electron-deficient cluster **1** at ambient temperature for 2 min, the initial green solution immediately turned orange and two compounds $[(\mu\text{-}H)Os_3(CO)_8(\mu\text{-}Cl)(\mu\text{-}dppm)]$ (**2**) and $[(\mu\text{-}H)Os_3(CO)_7(\eta^1\text{-}Cl)(\mu\text{-}Cl)_2(\mu\text{-}dppm)]$ (**3**) were isolated in 85% and 10% yields, respectively, after chromatographic separation. Both compounds **2** and **3** have been characterized by a combination of spectroscopic data and single-crystal X-ray diffraction analysis. An ORTEP diagram of the molecular structure of **2** is depicted in Fig. 1, crystal data are given in Table 1 and selected bond distances and bond angles are listed in Table 2. The molecule consists of a triangular cluster of osmium atoms with eight terminal carbonyl groups, one bridging chloride, one bridging hydride and a bridging dppm ligand. Three CO ligands are bound to Os(1) and Os(2) atom while Os(3) bears two carbonyls. The chloride and hydride

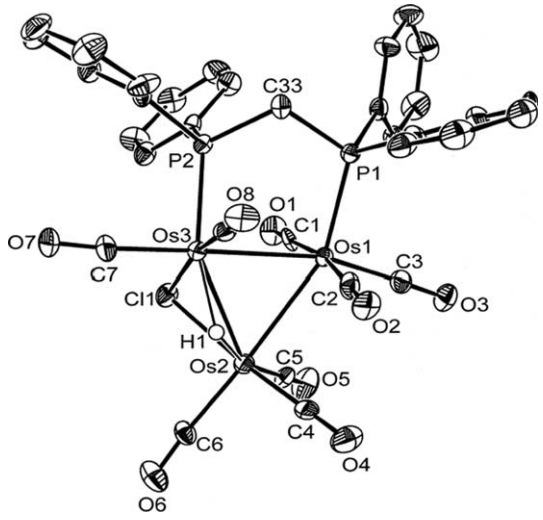

Fig. 1. Molecular structure of $[(\mu\text{-}H)Os_3(CO)_8(\mu\text{-}Cl)(\mu\text{-}dppm)]$ (**2**) showing the atom-labeling scheme. Thermal ellipsoids are drawn at the 50% probability level.

Table 1
Crystallographic data and structure refinement[a] for **2**, **3**, **4** and **6**

Compound	**2**	**3** · $0.25CH_2Cl_2$	**4**	**6** · $2CH_2Cl_2$
Formula	$C_{33}H_{23}ClO_8Os_3P_2$	$C_{32}H_{23}O_7Cl_3Os_3P_2 \cdot 0.25CH_2Cl_2$	$C_{33}H_{22}ClO_8Os_3P_2$	$C_{34}H_{23}F_3O_9Os_3P_2 \cdot 2CH_2Cl_2$
Formula weight	1215.50	1279.63	1214.50	1434.92
Crystal system	monoclinic	triclinic	monoclinic	orthorhombic
Space group	$P2_1/n$	$P\bar{1}$	$P2_1/n$	$P2_12_12_1$
a (Å)	15.6579(3)	10.8505(2)	16.32200(10)	9.9064(10)
b (Å)	12.7532(3)	11.7011(3)	10.8817(2)	15.9284(14)
c (Å)	17.1996(3)	16.4839(4)	20.6814(3)	26.663(2)
α (°)	90	89.3461(12)	90.0000(6)	90
β (°)	96.0695(8)	86.4453(12)	109.1381(5)	90
γ (°)	90	66.0351(8)	90.0000(9)	90
V (Å^3)	3415.32(14)	1908.53(8)	3479.23(8)	4207.2(7)
Z	4	2	4	4
D_{calc} (mg m^{-3})	2.364	2.227	2.325	2.265
μ (Mo Kα) (mm^{-1})	11.355	10.333	11.175	9.432
F(000)	2240	1181	2236	2672
Crystal size (mm)	$0.20 \times 0.15 \times 0.15$	$0.16 \times 0.12 \times 0.10$	$0.25 \times 0.22 \times 0.20$	$0.40 \times 0.24 \times 0.03$
θ Range (°)	3.05–27.49	3.10–27.53	2.97–27.51	1.49–28.38
Limiting indices	$-19 \leqslant h \leqslant 19$, $-16 \leqslant k \leqslant 16$, $-22 \leqslant l \leqslant 22$	$-14 \leqslant h \leqslant 14$, $-15 \leqslant k \leqslant 15$, $-21 \leqslant l \leqslant 21$	$-21 \leqslant h \leqslant 21$, $-14 \leqslant h \leqslant 14$, $-26 \leqslant l \leqslant 26$	$-13 \leqslant h \leqslant 13$, $-21 \leqslant k \leqslant 21$, $-35 \leqslant l \leqslant 35$
Number of reflections collected	28876	33332	53072	56672
Number of indepedent reflections (R_{int})	7747 (0.1045)	8683 (0.0774)	7941 (0.1146)	10502 (0.0610)
Maximum and minimum transmission	0.343 and 0.176	0.552 and 0.356	0.2134 and 0.1666	1.00 and 0.302505
Data/restraints/parameters	7747/0/424	8683/6/451	7941/0/424	10502/0/319
Goodness-of-fit on F^2	1.032	1.031	1.018	1.058
Final R indices [$I > 2\sigma(I)$]	$R_1 = 0.0445$, $wR_2 = 0.1021$	$R_1 = 0541$, $wR_2 = 0.1349$	$R_1 = 0.0568$, $wR_2 = 0.1486$	$R_1 = 0.0408$, $wR_2 = 0.0968$
R indices (all data)	$R_1 = 0.0445$, $wR_2 = 0.1021$	$R_1 = 0.0678$, $wR_2 = 0.1436$	$R_1 = 0.0746$, $wR_2 = 0.1555$	$R_1 = 0.0445$, $wR_2 = 0.0985$
Largest differecne in peak and hole (e Å^{-3})	2.138 and −2.355	9.631 and −3.216	11.522 and −6.132	2.141 and −1.348

[a] Details in common: X-radiation, Mo Kα ($\lambda = 0.71073$ Å), temperature (K) 150(2) except **6**, refinement method: full-matrix least-squares on F^2.

Table 2
Selected bond lengths (Å) and bond angles (°) for **2**

Os(1)–Os(2)	2.8298(4)	Os(1)–Os(3)	2.8390(4)
Os(2)–Os(3)	2.8572(5)	Os(2)–Cl(1)	2.482(2)
Os(1)–P(1)	2.325(2)	Os(3)–P(2)	2.324(2)
Os(3)–Cl(1)	2.450(2)		
Os(2)–Os(1)–Os(3)	60.5333(11)	P(2)–Os(3)–Os(1)	86.09(5)
P(2)–Os(3)–Os(2)	136.84(5)	P(1)–Os(1)–Os(2)	155.45(5)
P(1)–Os(1)–Os(3)	94.93(5)	Os(1)–Os(2)–Os(3)	59.893(11)
P(2)–Os(3)–Cl(1)	101.70(7)	Os(1)–Os(3)–Os(2)	59.574(11)
Os(2)–Cl(1)–Os(3)	70.82(5)	P(1)–C(33)–P(2)	112.3(4)
Cl(1)–Os(1)–Os(2)	54.07(5)	Cl(1)–Os(2)–Os(3)	55.11(5)
C(7)–Os(3)–Os(2)	117.9(3)	C(6)–Os(2)–Os(3)	115.6(3)

ligands bridge the same Os(2)–Os(3) edge but are located above and below the Os_3 plane (Fig. 1). The bridging hydride ligand was located but not refined. The Os–Os distances are very similar being in the range of 2.8298(4)–2.8572(5) Å. The dppm bridges the Os(1)–Os(3) vector with an angle of P(1)–C(33)–P(2) of 112.3(4)°. The Os(2)–Os(3) edge (2.8572(5) Å) which is mutually bridged by the chloride and the hydride ligands is comparable to the corresponding doubly bridged edge in [(μ-H)Os_3(CO)$_{10}$(μ-Cl)] {2.846(1) Å} [28]. The osmium–chloride bond distances are slightly asymmetrical, with Os(3)–Cl(1) = 2.450(2) Å and Os(2)–Cl(1) = 2.482(2) Å; the angle Os(2)–Cl(1)–Os(3) is quite acute, 70.82(5)°, which is similar to that observed in [(μ-H)Os_3(CO)$_{10}$(μ-Cl)] (70.83(9)°) [28]. The Os–P bond distances {2.325(2) and 2.324(2) Å} are comparable to the corresponding distances in [Os_3(CO)$_{10}$(μ-dppm)] [29]. The spectroscopic data for **2** are in accord with the solid-state structure. In agreement with the presence of the bridging hydride ligand on one of the Os–Os edges not bridged by the dppm ligand, the ^{1}H NMR spectrum of **2**, in the hydride region, shows a doublet at δ −12.88 with an H–P coupling constant of 31.6 Hz. The aliphatic region of the ^{1}H NMR spectrum contains two multiplets at δ 6.05 and 4.46 due to the two diastereotopic methylene protons of dppm ligand. Consistent with this, the ^{31}P{^{1}H} NMR spectrum exhibits two doublets at δ −18.1 and −22.5 (J = 25.5 Hz) due to two magnetically non-equivalent ^{31}P nuclei of the dppm ligand (see Scheme 1).

An ORTEP diagram of the molecular structure of **3** is shown in Fig. 2, crystal data are given in Table 1 and selected bond distances and bond angles are listed in Table 3. The molecule consists of an open cluster of three

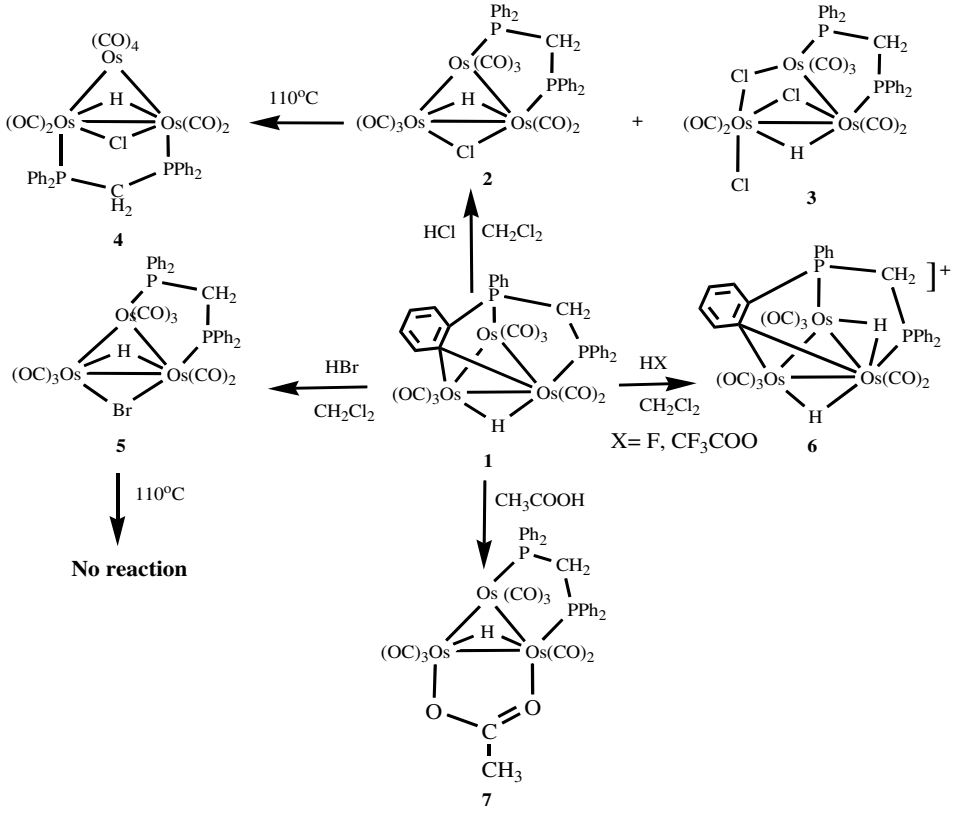

Scheme 1.

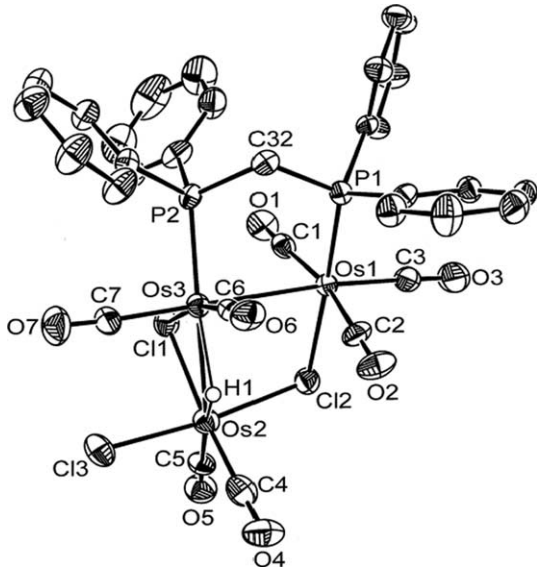

Fig. 2. Molecular structure of $[(\mu\text{-H})Os_3(CO)_7(\eta^1\text{-Cl})(\mu\text{-Cl})_2(\mu\text{-dppm})]$ (**3**) showing the atom-labeling scheme. Thermal ellipsoids are drawn at the 50% probability level.

Table 3
Selected bond lengths (Å) and bond angles (°) for **3**

Os(1)–Cl(2)	2.470(3)	Os(2)–Cl(3)	2.384(3)
Os(3)–P(2)	2.334(3)	Os(1)–P(1)	2.307(3)
Os(1)–Os(3)	2.9039(5)	Os(2)–Cl(2)	2.405(3)
Os(2)–Os(3)	2.9613(6)	Os(3)–Cl(1)	2.484(3)
Os(2)–Cl(1)	2.447(3)		
Cl(2)–Os(1)–Os(3)	84.55(6)	P(1)–Os(1)–Cl(2)	176.35(9)
Cl(3)–Os(2)–Cl(2)	173.10	P(1)–Os(1)–Os(3)	92.05(6)
P(2)–Os(3)–Os(1)	86.87(6)	Cl(3)–Os(2)–Cl(1)	87.64(11)
P(2)–Os(3)–Os(2)	153.79(7)	Cl(3)–Os(2)–Os(3)	90.78(8)
Os(1)–Os(3)–Os(2)	83.853(15)	Cl(1)–Os(2)–Os(3)	53.66(6)
Cl(1)–Os(3)–Os(1)	67.35(6)	Cl(1)–Os(3)–Os(2)	52.52(7)
Os(2)–Cl(2)–Os(1)	106.99(10)	Os(2)–Cl(1)–Os(3)	73.82(8)
P(2)–C(32)–P(1)	113.1(6)	C(6)–Os(3)–Os(2)	115.0(3)
Cl(2)–Os(2)–Os(3)	84.44(6)		

osmium atoms with two metal–metal bonds, seven terminal carbonyl groups and three chloride ligands, one edge of which is bridged by both a chloride and a hydride and other is bridged by the dppm ligand. The position of the hydride ligand was located but not refined. Osmium atoms Os(2) and Os(3) each have two terminal CO ligands but Os(1) has three. The Os(2)–Os(3) bond distance of 2.9613(6) Å is significantly longer than the Os(1)–Os(3) bond distance of 2.9039(5) Å but both are substantially longer than that of the corresponding Os–Os distances in **2** {2.8298(4)–2.8572(5) Å}. The Os(1)–Os(2) distance is very long at 3.919(4) Å and is clearly a non-bonding interaction. This open edge is asymmetrically bridged by a chloride ligand with Os–Cl bond distances of Os(1)–Cl(2) = 2.470(3) and Os(2)–Cl(2) = 2.405(3) Å. Another chloride ligand is terminally

coordinated to Os(2) with Os(2)–Cl(3) bond distance of 2.384(3) Å which is seen to be the shortest Os–Cl bond among the five. The Os(2)–Os(3) edge is spanned both by the chloride and hydride ligands lying above and below the Os_3 plane, respectively. The osmium–chloride bond distances are almost equal (Os(2)–Cl(1) = 2.497(3) and Os(3)–Cl(1) = 2.484(3) Å). The Os(2)–Cl(1)–Os(3) angle is quite acute {73.82(8)°} and is significantly smaller than the Os(2)–Cl(2)–Os(1) angle (106.99(10)°), but similar to the corresponding angle in [(μ-H)Os_3-$(CO)_{10}$(μ-Cl)] (70.83(9)°) [28]. The Os–P distances (2.307(3) and 2.334(3) Å) are similar to those in **2**. The spectroscopic data for **3** are in accord with the solid-state structure. The ^{1}H NMR spectrum in the hydride region shows a doublet of doublets at δ −12.66, indicating that the hydride is coupled to both non-equivalent ^{31}P nuclei. The aliphatic region of the spectrum contains two equally intense multiplets at δ 4.83 and 4.28 due to the methylene protons of the dppm ligand. Consistent with this the ^{31}P{^{1}H} NMR spectrum exhibits two doublets at δ −16.5 and −28.5 (J = 35.5 Hz) due to two magnetically non-equivalent ^{31}P nuclei of the dppm ligand. Compound **3** is a rare example of a structurally characterized triosmium cluster containing two bridging and one terminal chloride ligands. Most probably, this compound is formed from a further reaction of **2** with two moles of HCl followed by elimination of H_2 and rupture of a metal–metal bond.

Thermolysis of **2** in refluxing toluene at 110 °C resulted in a color change from orange to yellow and **4** was isolated in 60% yield after chromatographic separation. An ORTEP diagram of the molecular structure of **4** is shown in Fig. 3, crystal data are given in Table 1 and selected bond distances and bond angles are listed in Table 4. The molecule consists of a triangular cluster

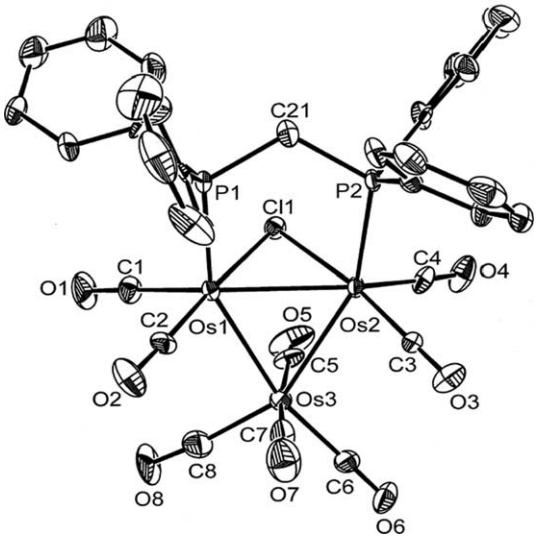

Fig. 3. Molecular structure of [(μ-H)Os_3(CO)$_8$(μ-Cl)(μ-dppm)] (**4**) showing the atom-labeling scheme. Thermal ellipsoids are drawn at the 50% probability level.

Table 4
Selected bond lengths (Å) and bond angles (°) for **4**

Os(1)–Os(2)	2.81498(5)	Os(1)–Os(3)	2.8241(6)
Os(2)–Os(3)	2.8276(6)	Os(2)–Cl(1)	2.489(2)
Os(1)–P(1)	2.350(3)	Os(2)–P(2)	2.354(3)
Os(2)–Cl(1)	2.485(2)		
Os(2)–Os(1)–Os(3)	60.190(14)	P(2)–Os(2)–Cl(1)	85.27(9)
Cl(1)–Os(2)–Os(1)	55.48(6)	P(1)–Os(1)–Os(3)	153.92(6)
P(1)–Os(1)–Os(2)	94.01(6)	P(1)–Os(1)–Cl(1)	83.16(8)
C(2)–Os(1)–Os(2)	121.2(3)	Cl(1)–Os(1)–Os(2)	55.59(6)
Os(1)-Os(3)–Os(2)	59.744(13)	C(3)–Os(1)–Os(2)	119.3(3)
P(2)–Os(2)–Os(1)	95.23(6)	P(2)–Os(2)–Os(3)	154.71(6)
Os(1)–Os(2)–Os(3)	60.067(14)	Os(1)-Cl(1)–Os(2)	68.93(6)
P(2)–C(21)–P(1)	119.9(10)	C(1)–Os(1)–Os(2)	142.6(3)

of osmium atoms bearing eight terminal carbonyl groups, one bridging chloride, one hydride and a dppm ligand. The Os–Os distances lie in the close ranges 2.8149(8)–2.8276(6) Å and do not show any differences between the bridged and unbridged edges. Two carbonyls are bonded to Os(1) and Os(2) whereas Os(3) is bonded to four carbonyls. An interesting feature of the structure of **4** is that the chloride and hydride span the same Os–Os vector as the dppm ligand. Although the position of the hydride ligand was not determined crystallographically, its presence in the same Os–Os edge as the chloride and dppm ligands was unambiguously verified by the ^{1}H NMR spectrum in the hydride region which contains a triplet at δ −12.74 with a H–P coupling constant of 12.8 Hz due to coupling to two equivalent ^{31}P nuclei. This conclusion is further supported by the arrangement of the carbonyl ligands, in particular the large C(2)–Os(1)–Os(2) angle of 121.2(3)° and C(3)–Os(1)–Os(2) angle of 119.3(3)° to accommodate the bridging hydride ligand. The feature of interest in **4** is the chloride ligand which symmetrically spans the Os(1)–Os(2) edge compared to that in **2**. Another example of a triosmium cluster having three bridging ligands on the same Os–Os edge is [(μ-H)Os_3(CO)$_8$(μ-OH)(μ-dppm)] [30]. A notable feature of **4** is that the P(1)–C(21)–P(2) bite angle is opened up considerably (120.0(6)°) compared to 112.3(4)° in **2** in order to make for room to accommodate the hydride and the chloride ligands inside the five-membered (Os(1)–Os(2)–P(2)–C(21)–P(1)) metallacycle during this transformation. That **4** is more thermodynamically stable than **2** probably reflects the net electron withdrawing effect of the HCl moieties on the Os(2)–Os(3) edge in **2**. The fact that **2** is the kinetic product suggests that its formation results from initial electrophillic attack on the Os–C bond of the μ-phenyl followed by nucleophillic attack by Cl^- on the same Os(2)–Os(3) edge.

A similar treatment of **1** with HBr gave [(μ-H)Os_3-(CO)$_8$(μ-Br)(μ-dppm)] (**5**) as the single product in almost quantitative yield. The structure of **5** is proposed from the spectroscopic data by analogy with **2**. The FAB mass spectrum shows the molecular ion peak at m/z 1260

corresponding to the formulation of $[(\mu\text{-H})Os_3(CO)_8(\mu\text{-Br})(\mu\text{-dppm})]$. The infrared spectrum of **5** is similar to that of **2** indicating that they have similar distribution of the carbonyl ligands. The ^1H NMR spectrum in the hydride region shows a doublet at δ −13.74 with a H–P coupling constant of 39.5 Hz. The resonance of the methylene protons of dppm is observed as two doublets of double doublets at δ 3.13 and 3.73, each integrating for 1 H. This arrangement of the ligands in **5** is strongly supported by the $^{31}P\{^1H\}$ NMR spectrum which shows two doublets at δ −19.1 and −22.9 (J = 39.5 Hz) due to the inequivalent phosphorus nuclei of the dppm ligand It is interesting that thermolysis of **5** in refluxing toluene at 110 °C does not convert it into an isomer in which the bromide and the hydride bridge the same Os–Os edge as the dppm ligand most probably because of steric reasons and the lower electronegativity of Br relative to Cl.

In sharp contrast, the reaction of **1** with HF results in an immediate color change from green to orange and only the cationic species $[(\mu\text{-H})_2Os_3(CO)_8(Ph_2PCH_2P(Ph)C_6H_4)]^+[CF_3O]^-$ (**6**) was isolated in almost quantitative yield after recrystallization from hexane/CH_2Cl_2 at room temperature. The molecular structure of cation **6** is shown in Fig. 4, crystal data are given in Table 1 and selected bond distances and bond angles are listed in Table 4. The structure consists of an Os_3 triangle with two shorter metal–metal bonds (Os(1)–Os(3) = 2.7673(5) and Os(2)–Os(3) = 2.8684(5) Å) and one significantly longer metal–metal bond (Os(1)–Os(2) = 3.0040(5) Å). The hydrides were located by using the program WinGX [31] and found to bridge Os(1)–Os(3) and Os(1)–Os(2) edges. The Os(1)–Os(2) edge is also bridged by the diphosphine ligand while the Os(1)–Os(3) edge is bridged by the metallated phenyl ring.

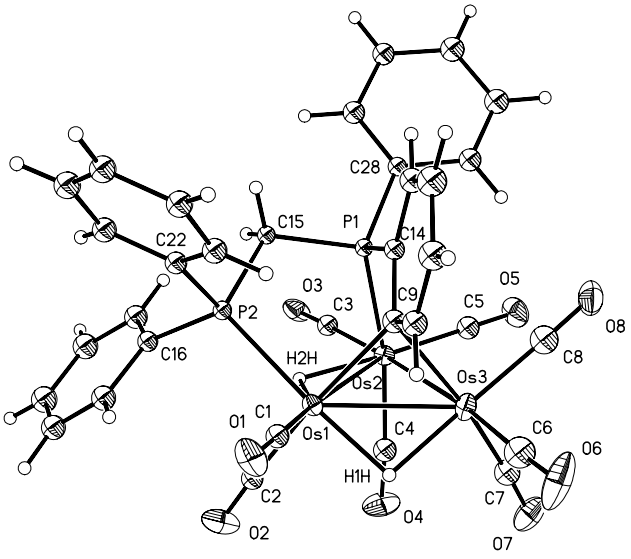

Fig. 4. Molecular structure of $[(\mu\text{-H})_2Os_3(CO)_8(Ph_2PCH_2P(Ph)C_6H_4)]^+$ (**6**) showing the atom-labeling scheme. Thermal ellipsoids are drawn at the 50% probability level.

Table 5
Selected bond lengths (Å) and bond angles (°) for **6**

Os(1)–P(2)	2.370(2)	Os(1)–H(1H)	1.8506
Os(2)–P(1)	2.364(2)	Os(1)–H(2H)	1.8574
Os(1)–Os(2)	3.0040(5)	Os(2)–H(2H)	1.8357
Os(2)–Os(3)	2.8684(5)	Os(3)–H(1H)	1.8516
Os(1)–Os(3)	2.7673(5)	F(1)–C(3S)	1.399(10)
F(3)–C(3S)	1.495(10)	C(3S)–O(1S)	1.277(13)
F(2)–C(3S)	1.456(10)	F–C(av.)	1.45(10)
Os(1)–C(9)	2.271(9)	Os(3)–C(9)	2.318(9)
P(2)–Os(1)–Os(3)	133.60(5)	P(2)–Os(1)–Os(2)	90.65(5)
Os(3)–Os(1)–Os(2)	59.437(12)	H(1H)–Os(1)–H(2H)	106.4
P(1)–Os(2)–Os(3)	87.02(5)	P(1)–Os(2)–Os(1)	75.42(5)
Os(3)–Os(2)–Os(1)	56.171(11)	Os(1)–Os(3)–Os(2)	64.392(13)
O(1S)–C(3S)–F(1)	118.8(8)	F(1)–C(3S)–F(2)	110.9(7)
O(1S)–C(3S)–F(2)	112.7(8)	F(1)–C(3S)–F(3)	103.2(7)
O(1S)–C(3S)–F(3)	108.6(8)	F(2)–C(3S)–F(3)	100.5(6)
O–C–F(av.)	113.36(7)	F–C–F(av.)	104.86(7)
P(1)–C(15)–P(2)	111.5(4)		

The Os(1)–Os(3) edge is comparable to the corresponding edge in **1** (2.747(1) Å) and is indicative of the unsaturated, 46-electron character of these triosmium clusters [15]. The Os(1) is ligated by two CO groups, while each of Os(2) and Os(3) is coordinated to three carbonyl ligands. The disposition of the metallated phenyl ring forces the phosphorus atoms of the diphosphine ligand to occupy axial co-ordination sites. A noticeable feature in the structure is that the metallated phenyl group forms asymmetric bridges across the Os(1)–Os(3) edge (Os(1)–C(9) = 2.271(9) and Os(3)–C(9) = 2.318(9) Å), in contrast to the parent cluster **1** in which there is no significant difference in the Os–C bond lengths for the bridging carbon atom of the metallated phenyl ring and probably reflects the electron withdrawing effect of protonation on the Os(1)–Os(2) edge [15]. The Os–P distances (Os(1)–P(2) = 2.370(2) and Os(2)–P(1) = 2.364(2) Å) are comparable to the corresponding distance in **1** (2.362(10) and 2.360(10) Å) [15]. The X-ray structure of this anion was first determined by Farnham et al. [32] as part of the complex $[(CH_3)_2N]_3S^+CF_3O^-$. Important bond lengths and angles of this anion are listed in Table 5. The average C–O and C–F distances (1.277(13) and 1.45(10) Å, respectively) and O–C–F and F–C–F angles (1.133(8) and 104.86°, respectively) are comparable to those reported previously [32]. This anion is most likely formed by the stepwise fluorination and hydrolysis (by trace moisture) of CH_2Cl_2. The conversion of chlorinated methanes to fluorinated alcohols by HF and water is well known [33].

Treatment of **1** with excess CF_3CO_2H in an NMR tube led to the formation of the protonated species $[(\mu\text{-H})_2Os_3(CO)_8(Ph_2PCH_2P(Ph)C_6H_4)]^+$. Its IR, ^1H and ^{31}P NMR spectroscopic data are very similar to those of the isolated **6** and $[(\mu\text{-H})_2Os_3(CO)_8(Ph_2PCH_2P(Ph)C_6H_4)]^+[BF_4]^-$. The latter was briefly described by Smith and co-workers [20] from the reaction of **1** with HBF_4 and characterized by spectroscopic data.

Since CF_3CO_2H and CH_3CO_2H are structurally similar but have different acidities, we investigated the reaction of **1** with CH_3CO_2H to see if **6** or an acid adduct is formed. Treatment of **1** with excess CH_3CO_2H for 15 days gave [(μ-H)Os_3(CO)$_8$(μ-η^2-CH_3CO_2)(μ-dppm)] (**7**) in 65% yield. Compound **7** has been characterized on the basis of spectroscopic data. The infrared spectrum of **7** in the terminal CO region is similar to that of **2** and **5** but it also exhibits two low energy absorption bands at 1964, and 1445 cm^1, which can be attributed to the –μ-η^2-CH_3CO_2 group [6]. Agreement between antisymmetric and symmetric carboxylate vibrations in **7** and those observed in [(μ-H)- Os_3(CO)$_{10}$(μ-η^2-CH_3CO_2)] and [(μ-H)Os_3(CO)$_{10}$(μ-η^2-HCO_2)], whose structure have been determined by X-ray diffraction studies, is excellent [34,35]. Its ^{1}H NMR in the hydride region shows a doublet of doublets at −9.18 with P–H coupling constants of 33.6 and 1.2 Hz, indicating that the hydride is bridging one of the Os–Os edges not bridged by the dppm ligand. The hydride chemical shift appears to be similar in related triosmium clusters containing bridging bidentate carboxylate moieties, [(μ-H)Os_3(CO)$_{10}$(μ-η^2-X)] ($\delta \sim -10$) [34,35]. The ^{31}P chemical shifts of **7** (δ −27.1 and −31.5; J = 39.2 Hz) are very similar to those of **2** and **5** indicating that they have related structures.

3. Conclusion

In this paper, we have demonstrated that the electronically unsaturated cluster **1** reacts with HCl gas to give two compounds, [(μ-H)Os_3(CO)$_8$(μ-Cl)(μ-dppm)] (**2**) and [(μ-H)Os_3(CO)$_7$(η^1-Cl)(μ-Cl)$_2$(μ-dppm)] (**3**), whereas with HBr it gives exclusively [(μ-H)Os_3-(CO)$_8$(μ-Br)(μ-dppm)] (**5**). In sharp contrast, HF reacts with **1** to give the protonated species [(μ-H)$_2$$Os_3$-(CO)$_8$($Ph_2PCH_2P(Ph)C_6H_4$)]$^+$ (**6**). This probably reflects the expected weaker μ-Os–F bond relative to the μ-Os–Cl and μ-Os–Br. Reaction of **1** with CF_3CO_2H also gives the cation **6** while reaction with CH_3CO_2H gives the adduct [(μ-H)Os_3(CO)$_8$(μ-η^2-CH_3CO_2)(μ-dppm)] (**7**) indicating that the basicity of the conjugate base also plays a role in determining the relative stability of simple protonation versus adduct formation. When refluxed in toluene at 110 °C both the hydride and chloride in **2** undergo edge migration to give **4** in which all the three ligands span the the same Os–Os edge. The formation of **2**, **5**, and **7** from **1** involves oxidative addition of HX followed by demetallation of the phenyl ring of the diphosphine ligand. It was not possible to convert **5** into the corresponding isomer of **4** suggesting that most probably the small bite of the dppm cannot accommodate the relatively large bromide ligand compared to chloride in **4**. Most interestingly, the acid adducts reported here all involve bridging modes for the acid anion. This is in sharp contrast to the previously reported acid adducts of the imidoyl species [(μ-H)Os_3(CO)$_9$(μ$_3$-η^2-C=NCH_2-CH_2CH_2–)X] (X = Cl, Br, CF_3CO_2, CF_3SO_2) where the anions are all terminally bonded to the cluster [13]. This is due to the facile reversibility of the orthometallation in **1** whereas CO loss (a much higher energy process) would be required to form μ-X adducts in the case of the imidoyls. This reversal of the orthometallation takes place even in the presence of relatively weak electron-donor, i.e., lone pairs on Cl, Br, and acetate.

4. Experimental

All the reactions were performed under a nitrogen atmosphere using standard Schlenk techniques. Solvents were dried and distilled prior to use by standard methods. Hydrogen fluoride and hydrogen bromide gas were purchased from Matheson gas products, Inc. while hydrogen choloride gas was purchased from Aldrich Chemical Company, Inc. The starting cluster [(μ-H)Os_3(CO)$_8$($Ph_2PCH_2P(Ph)C_6H_4$)] (**1**) was prepared according to the literature method [15]. Infrared spectra were recorded on a Shimadzu FT-IR 8101 spectrophotometer. ^{1}H and ^{31}P{^{1}H} NMR spectra were recorded on a Varian Unity Plus 400 and a Bruker DPX 400 spectrometers. Chemical shifts for the ^{31}P{^{1}H} NMR spectra are relative to 85% H_3PO_4.

4.1. Reaction of [(μ-H)Os_3(CO)$_8$($Ph_2PCH_2P(Ph)$-C_6H_4)] (1) with hydrogen chloride

HCl gas was bubbled through a CH_2Cl_2 solution (25 mL) of **1** (0.115 g, 0.098 mmol) at room temperature for 2 min during which time the color changed from green to orange. The solvent was removed under reduced pressure and the residue was chromatographed by TLC on silica gel. Elution with hexane/CH_2Cl_2 (1:1, v/v) gave two bands. The faster moving band afforded [(μ-H)-Os_3(CO)$_8$(μ-Cl)(μ-dppm)] (**2**) (0.101 g, 85%) as red crystals after recrystallized from hexane/CH_2Cl_2 at −4 °C. (Anal. Calc. for $C_{33}H_{23}ClO_8Os_3P_2$: C, 32.60; H, 1.91. Found: C, 32.81; H, 2.05%.) IR (ν(CO), CH_2Cl_2): 2078 s, 2029 m, 2004 vs, 1980 s, 1960 m, 1929 m cm^{-1}; ^{1}H NMR (CD_2Cl_2): δ 7.56 (m, 20H), 6.05 (m, 1H), 4.46 (m, 1H), −12.88 (d, 1H, J = 31.6 Hz); ^{31}P{^{1}H} (CD_2Cl_2): δ −18.1 (d), −22.5 (d, J = 45.5 Hz); mass spectrum: (m/z) 1214 [M]$^+$. The slower moving band afforded [(μ-H)Os_3(CO)$_7$(η^1-Cl)(μ-Cl)$_2$(μ-dppm)] (**3**) as pale yellow crystals (0.009 g, 7%) after recrystallization from hexane/CH_2Cl_2 at −4 °C. (Anal. Calc. for $C_{32}H_{23}O_7Cl_3Os_3P_2$: C, 30.54; H, 1.85. Found: C, 30.71; H, 1.98%.) IR [ν(CO), CH_2Cl_2]: 2093 w, 2049 m, 2029 m, 2010 vs, 1977 m, 1946 w cm^{-1}; ^{1}H NMR

(CD_2Cl_2): δ 7.46 (m, 20H), 4.03 (m, 1H), 4.80 (m, 1H), −12.57 (dd, 1H, J = 31.6, 4.8 Hz).

4.2. Thermolysis of **2**

A toluene solution (30 mL) of **2** (0.075 g, 0.062 mmol) was heated to reflux for 6 h. The solvent was removed under reduced pressure and the residue chromatographed by TLC on silica gel. Elution with hexane/CH_2Cl_2 (3:2, v/v) gave two bands. The first band gave unreacted **2** (0.012 g). The second band gave [(μ-H)Os_3-(CO)$_8$(μ-Cl)(μ-dppm)] (**4**) (0.045 g, 60%) as yellow crystals after recrystallized from hexane/CH_2Cl_2 at −4 °C. (Anal. Calc. for $C_{33}H_{23}ClO_8Os_3P_2$: C, 32.60; H, 1.91. Found: C, 32.75; H, 2.03%). IR [ν(CO), CH_2Cl_2]: 2080 s, 2006 vs, 1964 vw, 1943 w cm^{-1}; ^{1}H NMR ($CDCl_3$): δ 7.45–6.98 (m, 20H), 3.53 (m, 1H), 3.02 (m, 1H), −12.83 (t, 1H, J = 13.2 Hz); ^{31}P{^{1}H} NMR ($CDCl_3$): δ −10.4 (s).

4.3. Reaction of **1** with hydrogen bromide

HBr gas was bubbled through a CH_2Cl_2 solution (35 mL) of **1** (0.125 g, 0.106 mmol) at room temperature for 2 min during which time the color changed from green to orange. The solvent was then removed under reduced pressure and the residue chromatographed by TLC on silica gel. Elution with hexane/CH_2Cl_2 (1:1, v/v) gave one orange band which afforded [(μ-H)Os_3(CO)$_8$(μ-Br)(μ-dppm)] (**5**) (0.127 g, 95%) as red crystals after recrystallization from hexane/CH_2Cl_2 at −4 °C. (Anal. Calc. for $C_{33}H_{23}BrO_8Os_3P_2$: C, 31.45; H, 1.84. Found: C, 31.61; H, 1.96%.) IR (ν(CO), CH_2Cl_2): 2075 s, 2028 m, 2001 vs, 1982 s, 1958 s, 1929 m cm^{-1}; ^{1}H NMR ($CDCl_3$): δ 7.71–7.09 (m, 20H), 5.85 (m, 1H), 4.50 (m, 1H), −13.74 (d, 1H, J = 21.2 Hz); ^{31}P{^{1}H} ($CDCl_3$): δ −19.1 (d, J = 39.5 Hz), −22.9 (d, J = 39.5 Hz); mass spectrum: (m/z) 1260 [M]$^+$.

4.4. Reaction of **1** with hydrogen fluoride

HF gas was bubbled through a CH_2Cl_2 solution (35 mL) of **1** (0.106 g, 0.099 mmol) at room temperature for 2 min. The color immediately changed from green to orange. The solvent was removed under reduced pressure and the residue recrystallized from hexane/CH_2Cl_2 by slow evaporation of the solvent at room temperature to give [(μ-H)$_2$$Os_3(CO)_8$($Ph_2PCH_2P(Ph)C_6H_4$)]$^+$[$CF_3O$]$^-$ (**6**) (0.108 g, 99%) as orange crystals. (Anal. Calc. for $C_{33}FH_{23}O_8Os_3P_2$: C, 33.05; H, 1.94. Found: C, 33.21; H, 2.10%.) IR (ν(CO), CH_2Cl_2): 2101 s, 2072 m, 2061 s, 2031 m, 1999 s cm^{-1}; ^{1}H NMR (CD_2Cl_2): 9.07 (m, 1H), 8.19 (m, 1H), 7.73–7.56 (m, 10H), 7.37-7.28 (m, 3H), 7.03 (m, 1H), 6.81 (m, 2H), 4.68 (m, 1H), 3.47 (m, 1H) −13.75 (dd, 1H, J = 28.8, 7.1 Hz), −14.22 (J = 12.8, 4.4, 2.0 Hz). ^{31}P{^{1}H} ($CDCl_3$): δ −9.1 (d, J = 41.9 Hz), −18.3 (d, J = 41.9 Hz).

4.5. Reaction of **1** with CF_3CO_2H

CF_3CO_2H (one drop from a pauster pipette) was added to a CD_2Cl_2 solution (0.75 mL) of **1** (0.0.027 g, 0.106 mmol) in an NMR tube. The color immediately changed from green to orange. The ^{1}H and ^{31}P NMR indicated the formation of the protonated species [(μ-H)$_2$$Os_3(CO)_8$($Ph_2PCH_2P(Ph)C_6H_4$)]$^+$ (**6**). ^{1}H NMR (CD_2Cl_2): δ 9.07 (m, 1H), 8.17 (m, 1H), 7.75–7.49 (m, 10H), 7.40–7.29 (m, 3H), 7.04 (m, 1H), 6.96 (m, 1H), 6.74 (m, 2H), 4.47 (m, 1H), 3.34 (m, 1H) −13.74 (dd, 1H, J = 29.6, 8.0 Hz), −14.27 (J = 12.4, 4.0, 1.6 Hz). ^{31}P{^{1}H} NMR (CD_2Cl_2): δ −9.1 (d, J = 41.9 Hz), −18.3 (d, J = 41.9 Hz); ^{31}P{^{1}H} ($CDCl_3$): δ −8.7 (d, J = 41.9 Hz), −17.9 (d, J = 41.9 Hz).

4.6. Reaction of **1** with CH_3CO_2H

Glacial acetic acid (five drops from a pauster pipette) was added to a CH_2Cl_2 solution of **1** (0.022 g, 0.019 mmol) and allowed to stir at room temperature for 15 days during which time the color changed from green to yellow. The volatiles were removed under reduced pressure and the residue chromatographed by TLC on silica gel. Elution with hexane/CH_2Cl_2 developed a single band which afforded [(μ-H)Os_3(CO)$_8$(μ-η^2-CH_3CO_2)(μ-dppm)] (**7**) (0.015 g, 65%) as yellow crystals from hexane/CH_2Cl_2at −4 °C. IR (ν(CO), CH_2Cl_2): 2073 s, 2024 m, 1998 vs, 1975 s, 1948 s, 1922 m cm^1; (ν(COO), CH_2Cl_2): 1964 m, 1445 m cm^1; ^{1}H NMR ($CDCl_3$): δ 7.66-7.17 (m, 20H), 6.42 (ddt, 1H, J = 15.2, 10.0, 1.2 Hz), 4.64 (dt, 1H, J = 15.2, 12.0 Hz), −9.18 (dd, 1H, J = 33.6, 1.2 Hz); ^{31}P{^{1}H} ($CDCl_3$): δ −27.1 (d, J = 39.2 Hz), −31.5 (d, J = 39.2 Hz); mass spectrum: (m/z) 1238 [M]$^+$.

4.7. X-ray structure determination of **2**, **3**, and **4**

Single crystals of **2**, **3** and **4** suitable for X-ray diffraction were grown by slow diffusion of hexane into a dichloromethane solution at −4 °C. Crystallographic data were collected at 150 K, using a FAST area detector diffractometer and Mo Kα radiation (λ = 0.71073 Å). Data collection and processing were carried out using the programs COLLECT [36] and DENZO [37]. Empirical absorption corrections were applied to the data set using multiple and symmetry-related data measurements via the program SORTAV [38,39]. The unit cell parameters were determined from all observed reflections in a ϕ range of 3–10° and refined using the entire data set. The structures were solved by direct methods (SHELXS-97) [40] and refined on F^2 by full-matrix least-squares (SHELXL-97) [41] using all unique data. The bridging hydrides in **2** and **3** were located from a difference map but

not refined. All non-hydrogen atoms were refined anisotropically. The hydrogen atoms were included in calculated positions (riding model) with U_{iso} set at 1.2 times the U_{eq} of the parent atom. The crystals of compounds **3** and **4** grew as needles and although absorption corrections were made to the data, there were still large residual electron density peaks, 9.631 e $Å^{-3}$ in **3** which is located very close to the Os(2) atom with a distance 1.00 Å and 11.522 e $Å^{-3}$ in **4** which is located close to the Os(1) atom with a distance of 0.95 Å and have no chemical sense. We are as yet unable to obtain better quality crystals of **3** and **4**.

4.8. X-ray structure analysis of 6

Suitable crystals of **6** were coated with Paratone N oil, suspended in a small fiber loop, and placed in a cooled nitrogen gas stream at 173 K on a Bruker D8 SMART APEX CCD sealed tube diffractometer with graphite monochromated Mo Kα (0.71073 Å) radiation. A hemisphere of data was measured using a series of combinations of phi and omega scans with 10 s frame exposures and 0.3 frame widths. Data collection, indexing, and initial cell refinements were all carried out using SMART [42] software. Frame integration and final cell refinements were done using SAINT [43] software. The final cell parameters were determined from least-squares refinement on 7310 reflections. The SADABS [44] program was used to carry out absorption corrections.

The structures were solved using direct methods and difference Fourier techniques (SHELXTL-V6.12) [45]. Hydrogen atoms were placed in their expected chemical position using the HFIX command and were included in the final cycles of least squares with isotropic U_{ij}'s related to the atoms ridden on. The hydrides were positioned by using the XHYDEX program in the WinGX suite of programs [31]. All non-hydrogen atoms were refined anisotropically. Scattering factors and anomalous dispersion corrections are taken from the International Tables for X-ray Crystallography [46]. Structure solution, refinement, graphics, and generation of publication materials were performed by using SHELXTL-V6.12 software. The crystals of compound **6** grew as thin plates and although absorption corrections were made to the data, there were still large residual electron density peaks, ~2 e $Å^{-3}$ next to the osmium atoms. The other significant residual electron density in **6** was due to disorder of the CF_3O moiety which was not modeled. Additional details of data collection and structure refinement are given in Table 1.

Appendix A. Supplementary material

Crystallographic data for the structural analyses have been deposited with the Cambridge Crystallographic Data Centre, CCDC Nos. 265868 for compound **2**, 265869 for compound **3**, 265870 for compound **4**, and 265871 for compound **6.** Copies of this information may be obtained free of charge from The Director, CCDC, 12 Union Road Cambridge CB2 1EZ, UK (fax: +44 1223 336 033; email: deposit@ccdc.cam.ac.uk or www: http://www.ccdc.cam.ac.uk). Supplementary data associated with this article can be found, in the online version, at doi:10.1016/j.jorganchem.2005.03.041.

References

[1] (a) A.A. Koridze, O.A. Kizas, N.M. Astakhova, P.V. Petrovskii, Y.K. Grishin, J. Chem. Soc., Chem. Commun. (1981) 853;
(b) J. Knight, M.J. Mays, J. Chem. Soc. A (1970) 711;
(c) A.J. Deeming, B.F.G. Johnson, J. Lewis, J. Chem. Soc. A (1970) 2967.
[2] A.J. Deeming, S. Donovan-Mtunzi, S.E. Kabir, M.B. Hursthouse, K.M.A. Malik, N.P.C. Walker, J. Chem. Soc., Dalton Trans. (1987) 1869.
[3] A.J. Deeming, S.E. Kabir, J. Organomet. Chem. 340 (1988) 359.
[4] A.J. Deeming, K.I. Hardcastle, S.E. Kabir, J. Chem. Soc., Dalton Trans. (1988) 827.
[5] A.J. Deeming, S. Donovan-Mtunzi, K.I. Hardcastle, S.E. Kabir, K. Henrick, M. McPartlin, J. Chem. Soc., Dalton Trans. (1988) 579.
[6] G.R. Frauenhoff, S.R. Wilson, J.R. Shapley, Inorg. Chem. 30 (1991) 78.
[7] R.D. Adams, N.M. Golembeski, J.P. Selegue, Organometallics 1 (1982) 240.
[8] E.G. Bryan, W.G. Jackson, B.F.G. Johnson, J.W. Kelland, J. Lewis, K.T. Schorpp, J. Organomet. Chem. 108 (1976) 385.
[9] S.B. Colbran, P.T. Irele, B.F.G. Johnson, P.T. Kaye, J. Lewis, P.R. Raithby, J. Chem. Soc., Dalton Trans. (1989) 2033.
[10] A.J. Arce, A.J. Deeming, S. Donovan-Mtunzi, S.E. Kabir, J. Chem. Soc., Dalton Trans. (1985) 2479.
[11] E.J. Ditzel, B.F.G. Johnson, J. Lewis, J. Chem. Soc., Dalton Trans. (1989) 2033.
[12] M. Day, S.E. Kabir, E. Wolf, E. Rosenberg, K.I. Hardcastle, J. Cluster Sci. 9 (1990) 355.
[13] S.E. Kabir, E. Rosenberg, J. Stetson, M. Yin, J. Ciurash, K. Mnatsakanova, K.I. Hardcastle, H. Noorani, N. Movesesian, Organometallics 15 (1996) 4473.
[14] E. Rosenberg, Md.J. Abedin, D. Rokhsana, A. Viale, W. Dastru, R. Gobetto, L. Milone, K.I. Hardcastle, Inorg. Chim. Acta 334 (2002) 343.
[15] J.A. Clucas, D.F. Foster, M.M. Harding, A.K. Smith, J. Chem. Soc., Chem. Commun. (1984) 949.
[16] J.A. Clucas, M.M. Harding, A.K. Smith, J. Chem. Soc., Chem. Commun. (1985) 1280.
[17] M.P. Brown, P.A. Dolby, M.M. Harding, A.J. Mathews, A.K. Smith, J. Chem. Soc., Dalton Trans. (1993) 1671.
[18] K.A. Azam, M.B. Hursthouse, M.R. Islam, S.E. Kabir, K.M.A. Malik, R. Miah, C. Sudbrake, H. Vahrenkamp, J. Chem. Soc., Dalton Trans. (1998) 1097.
[19] M.P. Brown, P.A. Dolby, M.M. Harding, A.J. Mathews, A.K. ; Smith, D. Osella, D.M. Arbrun, R. Gobetto, P.R. Raithby, P. Zanello, J. Chem. Soc., Dalton Trans. (1993) 827.
[20] M.M. Harding, B. Kariuki, A.J. Mathews, A.K. Smith, P. Braunstein, P. J. Chem. Soc. Dalton Trans. (1994) 33.
[21] S.M.T. Abedin, K.A. Azam, M.B. Hursthouse, S.E. Kabir, K.M.A. Malik, M.A. Mottalib, E. Rosenberg, J. Cluster Sci. 12 (2001) 5.

[22] S.E. Kabir, K.M.A. Malik, E. Mollah, M.A. Mottalib, J. Organomet. Chem. 616 (2000) 157.
[23] S.E. Kabir, C.A. Johns, K.M.A. Malik, M.A. Mottalib, E. Rosenberg, J. Organomet. Chem. 625 (2001) 112.
[24] S.E. Kabir, S. Pervin, N.C. Sarker, A. Yesmin, A. Sharmin, T.A. Siddiquee, D.T. Haworth, D.W. Bennett, K.M.A. Malik, J. Organomet. Chem. 681 (2003) 237.
[25] S.M.T. Abedin, K.I. Hardcastle, S.E. Kabir, K.M.A. Malik, M.A. Mottalib, E. Rosenberg, M.J. Abedin, Organometallics 19 (2000) 5623.
[26] A.J. Deeming, M.M. Hassan, S.E. Kabir, E. Nordlander, D.A. Tocher, J. Chem. Soc., Dalton Trans. (2004) 3079.
[27] (a) S.E. Kabir, K.M.A. Malik, H.S. Mandal, M.A. Mottalib, M.J. Abedin, E. Rosenberg, Organometallics 21 (2002) 2593;
(b) S.M.T. Abedin, T. Akter, N. Begum, S.E. Kabir, M.A. Miah, M.A. Mottalib, D. Rokhsana, E. Rosenberg, G.M.G. Hossain, K.I. Hardcastle, Organometallics (in preparation).
[28] M.R. Churchill, R. Lashewycz, Inorg. Chem. 18 (1979) 1926.
[29] K.A. Azam, M.B. Hursthouse, S.E. Kabir, K.M.A. Malik, M.A. Mottalib, J. Chem. Crystallogr. 29 (1999) 813.
[30] S.R. Hodge, B.F.G. Johnson, J. Lewis, P.R. Raithby, J. Chem. Soc., Dalton Trans. (1987) 931.
[31] L.J. Farrugia, J. Appl. Crystallogr. 32 (1999) 837.
[32] W.R. Farnham, B.G. Smart, W.J. Middleton, W.J. Calabrese, D.A. Dixon, J. Am. Chem.. Soc. 107 (1985) 4565.
[33] G. Kloter, K. Seppelt, J. Am. Chem. Soc. 101 (1979) 347.
[34] P.M. Lausarot, G.A. Vaglio, M. Valle, A. Tiripicchio, M.T. Camellini, P.J. Gariboldi, J. Organomet. Chem. 291 (1985) 221.
[35] E.G. Bryan, B.F.G. Johnson, J. Lewis, J. Chem. Soc., Dalton Trans. (1977) 1328.
[36] R. Hooft, COLLECT: Data Collection Software, Nonius B.V., Delft, The Netherlands, 1998.
[37] Z. Otwinowski, W. Minor, in: C.W. CarterJr., R.M. Sweet (Eds.), Macromolecular Crystallography, Academic Press, New York, 1997, pp. 307–326.
[38] R.H. Blessing, Acta Crystallogr., Sect. A 51 (1995) 33.
[39] R.H. Blessing, J. Appl. Crystallogr. 30 (1997) 421.
[40] G.M. Sheldrick, Acta Crystallogr., Sect. A 46 (1990) 467.
[41] G.M. Sheldrick, SHELXL-97: Program for Crystal Structure Refinement, University Göttingen, Göttingen, Germany, 1997.
[42] SMART Version 5.628, Bruker AXS, Inc., Madison, WI, 2003.
[43] SAINT Version 6.36, Bruker AXS, Inc., Madison, WI, 2002.
[44] G. Sheldrick, SADABS Version 2.10, University of Göttingen, Göttingen, Germany, 2003.
[45] SHELXTL-V6.12, Bruker AXS, Inc., Madison, WI, 2003.
[46] A.J.C. Wilson (Ed.), International Tables for X-ray Crystallography, vol. C, Kynoch Press/Academic Publishers, Birmingham/Dordrecht, 1992, Tables 6.1.1.4 (pp. 500–502) and 4.2.6.8 (pp. 219–222).